Int. J. Heat Mass Transfer. Vol. 29, No. 12, pp. 1903–1909, 1986
Printed in Great Britain

0017–9310/86 $3.00 + 0.00
Pergamon Journals Ltd.

Heat transfer and pressure drop on the shell-side of tube-banks having oval-shaped tubes

G. P. MERKER and H. HANKE
Institut für Technische Thermodynamik und Kältetechnik der Universität Karlsruhe (TH), F.R.G.

(*Received* 20 *January* 1986)

Abstract—Heat transfer and pressure drop of the cross-flow on the shell-side of staggered tube-banks, having different transversal and longitudinal pitches in the range of $1.97 \leqslant t_q \leqslant 3.16$ and $0.67 \leqslant t_l \leqslant 1.0$, respectively, have been studied experimentally. The heat transfer was determined with the aid of the analogy between heat and mass transfer from measurements of the mass diffusion of naphthalene. The results show that exchangers with oval-shaped tubes have considerably smaller front areas on the shell-side compared to those with circular tubes.

1. INTRODUCTION

IN RECENT years, the question of recovering heat from waste gas has been considered by using cross-flow, oval-shaped exchangers rather than conventional ones with circular tubes. Tube-banks with oval-shaped tubes require considerably less pumping power on the shell-side than those with circular tubes. In other words, the resulting frontal area on the shell-side is much lower and the overall design more compact assuming that the pumping power is kept constant. Therefore, oval-shaped tube-banks are advantageous when a very compact design with a very low pressure drop on the shell-side is required. Up to now, only a relatively small amount of experimental results on cross-flow heat exchangers with staggered oval-shaped tubes have been published. Winding and Cheney [1] have studied the mass transfer of test-tubes made of naphthalene and having circular and drop-shaped tubes. Brauer [2] measured the heat transfer rate in cross-flow tube-banks with circular, oval and more complicated shaped tubes. Very recently, Ruth [3] has reported on measurements of the heat transfer rate and the pressure drop in cross-flow tube-banks having lenticular tubes in a staggered arrangement.

2. EXPERIMENTAL SET-UP

The study has been carried out with the aid of an open wind-tunnel. Figure 1 shows a schematic sketch of the experimental set-up. Air is sucked in by a fan and pumped through the heating section where the temperature of the air stream is controlled. The adjustable heating elements allow a temperature constancy of ± 0.1 K. Inside the adjacent stabilization chamber five wire grids are mounted to control the turbulence level of the air flow and to produce a uniform velocity profile in the entrance cross-section of the test section. Having passed the test section, the air stream leaves the wind-tunnel via the exhaust pipe.

The test section has a free flow area of 120×160.4 mm^2 and a length of 720 mm. The tube-banks inserted into the test section may not be longer than 300 mm. Eight static pressure taps equally distributed over the circumference in the entrance and exit cross-section of the test section allow the evaluation of the static pressure in each of these cross-sections and, hence, the pressure drop over the test section may be determined. In addition, two total head tubes adjustable over each of the cross-sections allow the dynamic pressure and, hence, the resulting velocity profiles in front and behind the tube-bank to be measured. Quick-acting clamps on the top and bottom wall of the test section allow for a fast assembly and disassembly of a single naphthalene test tube as well as of the complete tube-bank.

The fan is adjusted with the aid of the bypass valve Bp 1 and via variable transformers. The air-velocity in the free flow area of the test section can be varied between 0.3 and 30 m s^{-1}. The turbulence intensity

$$Tu = \frac{\sqrt{|u'|^2}}{\bar{u}} \tag{1}$$

of the entering air flow in front of the test section was as low as 0.05% regardless of the air velocity. About 2 cm behind the last row of the tube-bank the turbulence intensity had a value of 1% when measured in the wake region between two tubes and of 2.5% just behind one tube. Figure 2 shows the outlay and the characteristic dimensions of a tested tube-bank. The relative longitudinal pitches were 1.00, 0.83 and 0.67, and the relative transversal pitches 1.97, 2.26, 2.63 and 3.16. To avoid a bypass stream between the tube-bank and the side wall of the test section, half the oval-shaped tubes were fixed on the side wall at each second row. The oval-shaped tubes had a long chord of 30.2 mm and a short one of 7.6 mm. The circumference of the oval-shaped tubes was composed of two arcs of a circle having different radii.

NOMENCLATURE

A	wetted surface area of one tube [m^2]
A_a	wetted surface area of the tube-bank [m^2]
A_c	minimum free flow area [m^2]
A_f	frontal area [m^2]
L_c	characteristic length [m]
m	mass [kg]
Δm	mass loss [kg]
N_R	number of tube-rows arranged in streamline
p_{stat}	static pressure [$N\,m^{-2}$]
Δp_{stat}	pressure drop [$N\,m^{-2}$]
$\dot{Q}$	thermal power (duty) [$kJ\,s^{-1}$]
s_l	distance from side of oval-shaped tube to center line of adjacent tube in next row [m]
s_2	minimum distance between oval-shaped tube and adjacent tube in next row [m]
s_e	effective minimum distance between two rows [m]
s_l	longitudinal tube spacing [m]
s_q	transversal tube spacing [m]
t	time [s]
t_l	relative longitudinal pitch [m]
t_q	relative transversal pitch [m]
Tu	turbulence intensity
U	circumference of oval-shaped tube [m]
$\bar{u}$	average stream velocity [$m\,s^{-1}$]
u'	fluctuation of stream velocity [$m\,s^{-1}$]
w_c	characteristic stream velocity [$m\,s^{-1}$]
w_e	nominal maximum velocity calculated from minimum area [$m\,s^{-1}$].

Greek symbols

ξ	drag coefficient
ρ_w	density of naphthalene vapor at tube surface [$kg\,m^{-3}$]
ρ_∞	density of naphthalene vapor in free stream [$kg\,m^{-3}$]
ψ	void fraction.

Transport coefficients

D	naphthalene air diffusion coefficient [$m^2\,s^{-1}$]
α	heat transfer coefficient [$W\,m^{-2}\,K^{-1}$]
β	mass transfer coefficient [$m\,s^{-1}$]
λ	thermal conductivity [$W\,m^{-1}\,K^{-1}$]
κ	thermal diffusivity [$m^2\,s^{-1}$]
ν	kinematic viscosity [$m^2\,s^{-1}$].

Dimensionless numbers

Le	Lewis number, $Sc/Pr = K/D$
Nu	Nusselt number, $\alpha L_c/\lambda$
Pr	Prandtl number, ν/x
Re	Reynolds number, $w_c L_c/\nu$
Sc	Schmidt number, ν/D
Sh	Sherwood number, $\beta L_c/D$.

3. EXPERIMENTAL TECHNIQUE

Direct measurements of the heat transfer rate in tube-banks require considerable experimental effort. Furthermore, the tube-banks have to be leakproof for direct measurements, since the working fluid flows on the tube-side as well as on the shell-side. For this reason, the heat transfer was determined with the aid of the analogy between heat and mass transfer from measurements of the mass diffusion of naphthalene in air using test-tubes made of naphthalene. In all test runs only one tube of the bank was replaced by a naphthalene tube. This test-tube was always positioned in the middle of a tube row. The test-tubes were produced through pressing naphthalene powder in dividable press moulds. The density of the pressed naphthalene was equal to that of crystalline; see Presser [4].

With the mass loss Δm of the test-tube during the test time Δt one obtains for the mass transfer

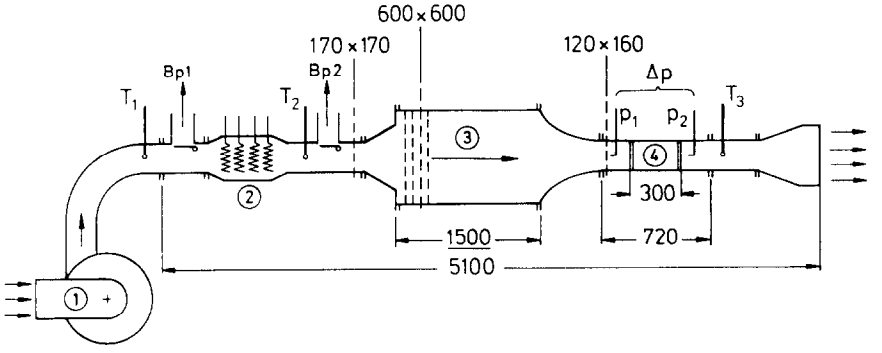

FIG. 1. Schematic sketch of the experimental set-up: 1, fan; 2, heating section; 3, stabilization chamber; 4, test section.

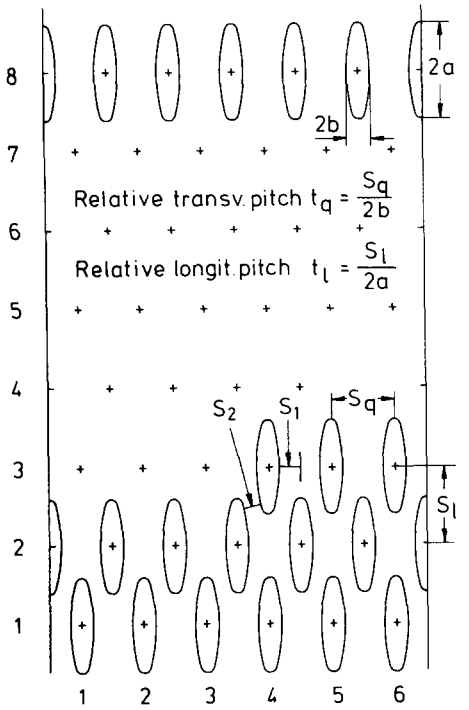

FIG. 2. Typical arrangement of a tube-bank.

coefficient

$$\beta = \frac{\Delta m}{\Delta t A(\rho_w - \rho_\infty)} \tag{2}$$

where A is the effective surface area for the mass transfer process. The density of the naphthalene vapour at the wall, ρ_w, is obtained from the ideal gas law, namely, determining the partial pressure of naphthalene on the surface at surface temperature. Since the sublimation process of naphthalene into air progresses approximately isothermally, due to the very low sublimation heat of naphthalene (see Presser [4] and Cur and Sparrow [5]), the surface temperature of the naphthalene tube can be set equal to the temperature of the air flow and, hence, the partial pressure of the naphthalene equal to the vapour pressure at the surface temperature. The effect of the humidity on the mass transfer can be neglected; see Sparrow and Niethammer [6].

The average mass loss during a test run was about 100 mg at a total weight of the naphthalene test-tube of about 38 g. The test time varied between 15 and 60 min depending on the air flow rate, $\dot{V}$.

With a characteristic length L_c and the diffusion coefficient D of naphthalene one obtains for the Sherwood number

$$Sh = \frac{\beta L_c}{D}. \tag{3}$$

Using the analogy between heat and mass transfer, the Sherwood number can be transferred into a Nusselt number. This yields

$$Nu = Sh \cdot Le^{-n} \tag{4}$$

where the Nusselt and Lewis numbers are defined as

$$Nu = \frac{\alpha L_c}{\lambda} \tag{5}$$

$$Le = \frac{Sc}{Pr} = \frac{\kappa}{D}. \tag{6}$$

By comparing forced convection heat transfer experiments for fluids with different Prandtl numbers obtained on single tubes with elliptical cross-sections and a chord radio of 4:1, Zukauskas and Ziugszda [7] found the exponent n in equation (4) to have a value of 0.37. The Sherwood and Nusselt numbers are usually shown as a function of the Reynolds number

$$Re = \frac{w_c L_c}{\nu} \tag{7}$$

where L_c is again the characteristic length and w_c the characteristic velocity of the tube-bank. It can be shown that a reasonable measure of the characteristic velocity is the velocity in the minimum free-flow area which is either between two tubes in the same row or between two tubes in adjacent rows depending on the relative longitudinal pitch. Following Gnielinski [8] and Kast *et al.* [9], the streamed length has been chosen as the characteristic length in equations (3), (5) and (7). For the oval-shaped tubes used in these experiments the streamed length was determined to be 31.6 mm.

4. EXPERIMENTAL RESULTS

4.1. *Mass transfer*

The tube-banks used in the mass transfer experiments were composed of eight tube rows in the main flow direction. For each test run only one tube of the bank was replaced by a naphthalene test-tube, this tube was arranged in the middle of a tube row. For the design with $t_l = 1.0$ and $t_q = 1.97$, Fig. 3 shows the resulting Sherwood number for each row of the bank. In this figure the data are connected by straight lines which do not have any physical meaning. For low Reynolds numbers, below 3000, the Sherwood number has approximately the same value in each row. By increasing the Reynolds number up to values of about 20 000 the velocity field inside the tube-bank obviously experiences some changes. Therefore, the Sherwood number increases from the first to the third row, decreases then down to the fifth or the sixth row, and increases again up to the last row. Taking the scattering of the experimental data into account, the Sherwood number may be taken as fairly constant from the fourth or fifth row until the last one, i.e. the entrance region is restricted to the first three or four

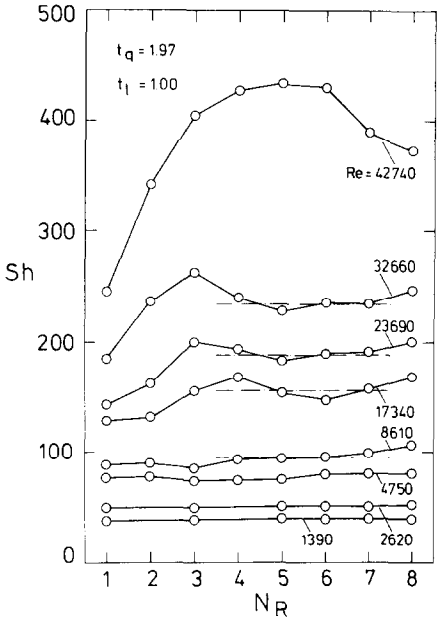

FIG. 3. Sherwood number vs row number for the tube-bank with $t_q = 1.97$ and $t_l = 1.0$.

rows of the bank. For the largest Reynolds number of about 43 000, noise production was recorded. The completely different data curve in this case makes it clear that the velocity field in the bank undergoes drastic changes as soon as noise production occurs, see also Section 4.2. The onset of noise was recorded in each bank as soon as the Reynolds number went beyond a certain value. Figure 4 shows the Sherwood number vs Reynolds number for eight banks having different longitudinal and transversal pitches. The Sherwood number shown is the arithmetic mean value between the fourth and the seventh row. It is interesting to note that the data of the Sherwood numbers for banks having the same longitudinal pitch are very close together and may be represented by just one empirical correlation, i.e. the relative transversal pitch has a very weak influence. Considering banks with longitudinal pitches of 1.0, one sees that the flow-field and, hence, the Sherwood/Reynolds number dependence, changes when the Reynolds number surpasses a value of about 6400.

For banks with $t_l = 1.0$ the data can be represented by a simple empirical correlation of the form

$$Sh = 1.181 \cdot Re^{0.480}, \quad Re < 6400 \tag{8}$$

$$Sh = 0.212 \cdot Re^{0.676}, \quad Re > 6400. \tag{9}$$

The Reynolds number, where the two regions intersect, is shifted down to lower values if the relative longitudinal pitch is reduced. However, for banks with a longitudinal pitch of $t_l = 0.67$ no such intersection point could be determined inside the Reynolds number region considered in the present study. For these banks the data can be correlated by

$$Sh = 0.442 \cdot Re^{0.622}. \tag{10}$$

Furthermore, Fig. 4 shows the correlation for a single oval-shaped tube. Comparing the correlations for this tube with those for the tube-banks, it is obvious that the mass transfer coefficient for the tube-banks is clearly better if the longitudinal pitch is smaller than

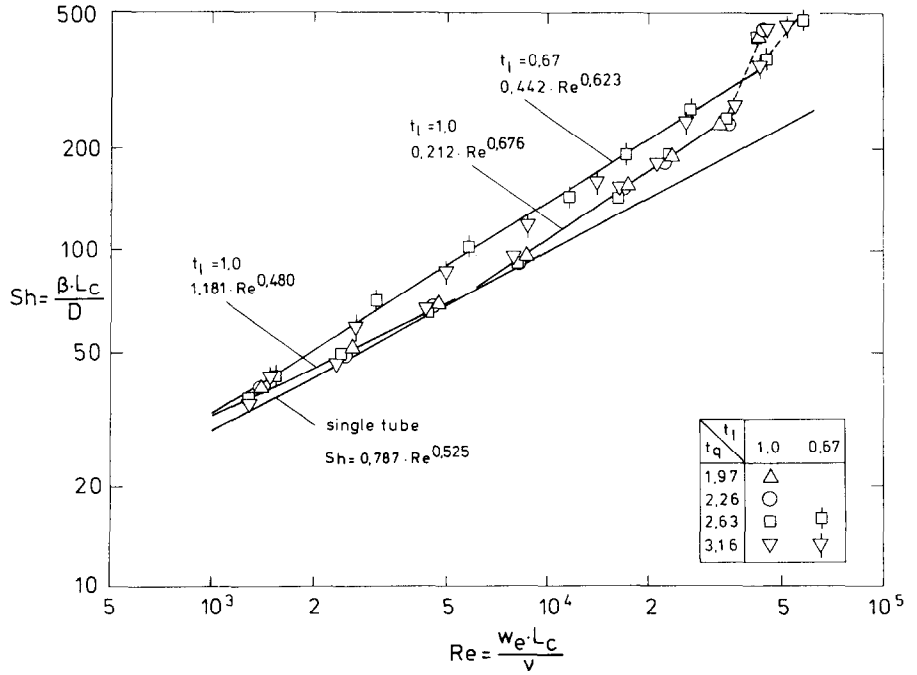

FIG. 4. Sherwood number vs Reynolds number for a single tube as well as for six different tube-banks.

$t_l = 1.0$. For $t_l = 1.0$ the Sherwood number is only distinctly better if the Reynolds number is sufficiently high.

4.2. *Pressure drop*

Figure 5 presents the results of the pressure loss measurements for banks with eight rows and a longitudinal pitch of 1.0. The diagram shows the ratio of pressure loss, Δp_{stat}, to the dynamical pressure of the free stream vs Reynolds number. It can be seen that the pressure drop increases with decreasing relative transversal pitch, and it decreases with increasing Reynolds number. At a certain Reynolds number a weak noise production is recorded which disappears completely as soon as the Reynolds number slightly increases. As already mentioned, however, further increasing of the Reynolds number results in a serious noise production which is coupled with a drastic rise in pressure drop. A characteristic feature of this noise production is that the frequency of the noise is independent of the Reynolds number and also of the transversal pitch, the value measured is about 1000 Hz. The same holds also for banks with longitudinal pitches lower than 1.0. This behaviour can be fairly well described by assuming a standing wave perpendicular to the main flow direction.

The influence of the numbers of rows on the pressure drop was carried out by successive reduction of the number of rows from eight to at least one. Figure 6 shows the pressure drop Δp_{stat} divided by the number of rows N_R and by the dynamic pressure of the free stream vs the row number for a Reynolds number of 15000. We would like to make it clear that this graph does not show the specific pressure drop of a certain row but rather the average pressure drop per row for a bank having N_R rows. For the bank with $t_l = 1.0$ the relative average pressure drop per row decreases with increasing row numbers. Besides the weak

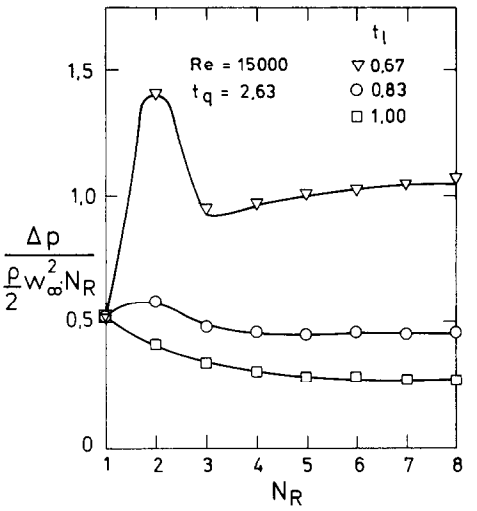

FIG. 6. Modified pressure drop vs row number for tube-banks with $t_q = 2.63$ for a Reynolds number of 15000.

increase in pressure drop for a bank with two rows, the same holds for the longitudinal pitch $t_l = 0.83$. For these two pitches the cross-flow in the bank may be considered as fully developed behind the fifth row. In comparison, the graph for the bank with $t_l = 0.67$ is quite different. The average pressure drop has a maximum for a bank with two rows and a minimum for one with three rows. The reason for this may be that the separation point of the boundary layer on the oval-shaped tubes of the first row is pushed further downstream if a second row is added. Due to this the minimum free-flow area between the first and the second row is further reduced by the relative thickness of the boundary layer on the tubes of the first row. Hence, the effective flow velocity is increased and the pressure drop rises. Adding a third row leads to early

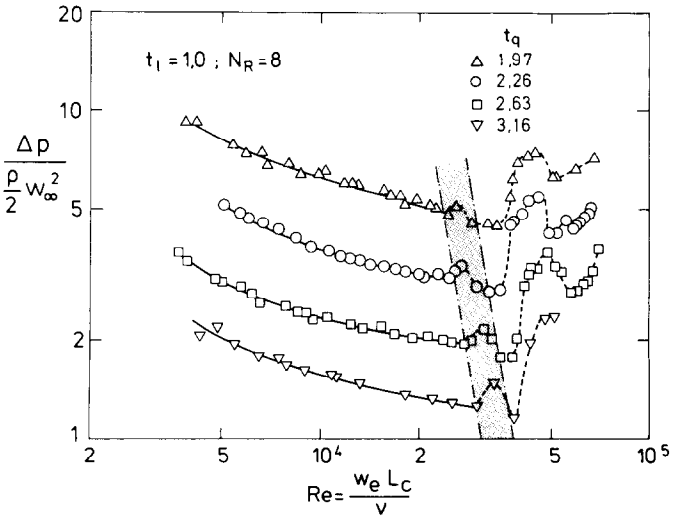

FIG. 5. Pressure drop vs Reynolds number for tube-banks with $t_l = 1.0$.

separation of the boundary layer on the tubes in the second row. Although the boundary layer is reattached further downstream the whole flow field is different. However, the average pressure drop is increased if additional tube rows are added to the bank and the flow may be considered as fully developed behind the sixth or seventh row.

To define a pressure loss coefficient, we consider a mechanical energy balance for the whole tube-bank

$$\dot{V} \cdot \Delta p_{\text{stat}} = A_a \frac{\rho w_c^2}{2} \xi w_c. \tag{11}$$

The LHS of equation (11) represents the pumping power necessary to get the air through the tube-bank. The RHS states that this pumping power is proportional to the dynamic pressure $\rho w_c^2/2$, the wetted surface of the bank and the characteristic velocity w_c. If one chooses as characteristic velocity the nominal maximum velocity calculated from the minimum flow area between the tubes one obtains from equation (11) for the pressure drop coefficient

$$\xi = \frac{\Delta p_{\text{stat}}}{\rho w_\infty^2/2} \frac{A_e^3}{A_f^2 A_a}. \tag{12}$$

Instead of the flow areas A_e and A_f we can use the pitch s_q and the minimum distance s_e between two tubes and obtain

$$\xi = \frac{\Delta p_{\text{stat}}}{\rho w_\infty^2/2} \frac{s_e^3}{s_q^2 U} \frac{1}{N_R} \tag{13}$$

with

$$s_e = \begin{cases} 2s_1 & \text{for } t_l = 1.0 \\ 2s_2 & \text{for } t_l \leqslant 0.83. \end{cases}$$

The length U is the circumference of a single tube.

Figure 7 presents the drag coefficient (ξ) vs Reynolds number (Re) for tube-banks with eight rows having different longitudinal and transversal pitches, t_l and t_q. The figure shows that the drag coefficient is nearly independent of the relative transversal pitches of the tube-banks. Hence, drag coefficients for tube-banks having identical longitudinal pitches but different transversal pitches can be represented by one correlation. One obtains

$$\xi = K \cdot Re^m \tag{14}$$

t_l	K	m	
1.0	1.668	−0.479	$Re < 7500$
1.0	0.216	−0.250	$Re > 7500$
0.67	0.691	−0.359	$Re < 10000$
0.67	0.251	−0.250	$Re > 10000$

The mean deviation of the data from the correlation equation is about $\pm 6\%$.

5. COMPARISON OF DIFFERENT HEAT EXCHANGER CONFIGURATIONS

The main difference between tubular cross-flow heat exchangers having circular or oval-shaped tubes becomes clear from Fig. 8. This diagram shows the ratio of the thermal power per unit temperature to the pumping power vs the mass flow rate. Only the flow on the shell-side is taken into account. For this comparison, the wall temperature, the overall size of the exchanger, the total heat transfer surface, and the void fraction are held constant. The lines of Fig. 8 relate to three circular tube-banks and one oval-shaped tube-bank. Each of the three circular tube-banks consists of 168 tubes, but the overall design is different, i.e. the bundles have 24, 14 and 7 rows in the main stream direction, respectively. The graphs show that the ratio ε is greater the larger the frontal area of the shell-side is. This feature of circular tube-arrangements is well known and leads to the so-called 'towel-like' design of this type of exchanger. Considering the curve valid for the oval-shaped tube-bank, it can be seen that its

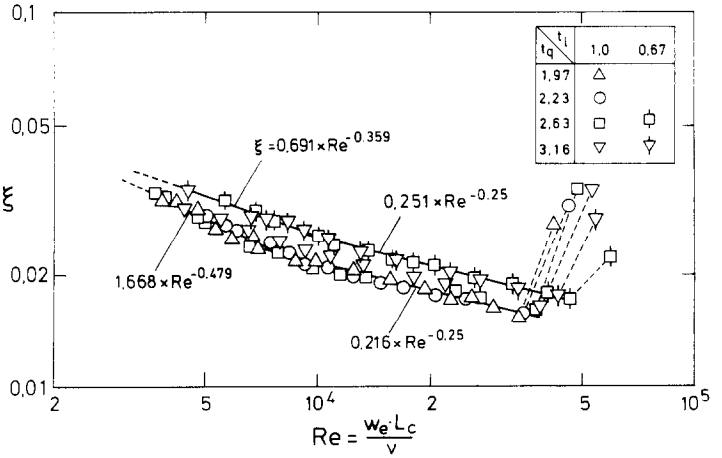

FIG. 7. Drag coefficient vs Reynolds number for six different tube-banks.

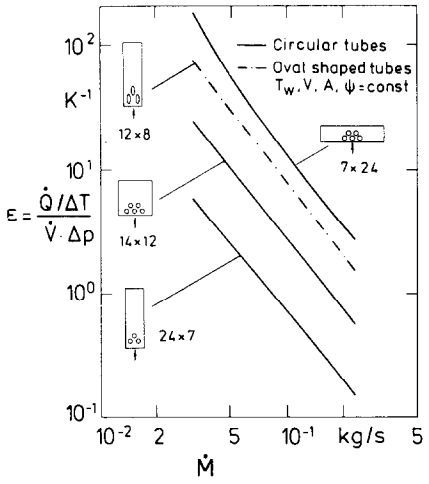

FIG. 8. Ratio of thermal power per unit temperature to the pumping power vs mass flow rate for tube-banks with circular and oval-shaped tubes.

frontal area is much smaller than that of the circular tube-bank in question. From this feature we conclude that, in general, oval-shaped tube-banks have small frontal areas on the shell-side compared to those with circular tubes. This is advantageous when the available pumping power on the shell-side is restricted as is usually the case in waste heat recovery from the exhaust of gas turbines.

REFERENCES

1. C. C. Winding and A. J. Cheney, Jr., Mass and heat transfer in tube banks, *Int. Engng Chem.* **40,** 1087–1093 (1948).
2. H. Brauer, Untersuchungen an Querstrom-Wärmeaustauschern mit verschiedenen Rohrformen, *Mannesmann-Forschungsber.* **126,** 3–18 (1961).
3. E. K. Ruth, Experiments on a crossflow heat exchanger with tubes of lenticular shape, *J. Heat Transfer* **105,** 571–575 (1983).
4. K. H. Presser, Experimentelle Prüfung der Analogie zwischen konvektiver Wärme und Stoffübertragung bei nicht abgelöster Strömung, *Wärme- u. Stoffübertr.* **1,** 225–236 (1968).
5. N. Cur and E. M. Sparrow, Experiments on heat transfer and pressure drop for a pair of colinear interrupted plates aligned with the flow, *Int. J. Heat Mass Transfer* **21,** 1069–1080 (1978).
6. E. M. Sparrow and J. E. Niethammer, Natural convection in a ternary gas mixture—application to the naphthalene sublimation technique, *J. Heat Transfer* **101,** 404–410 (1979).
7. A. Zukauskas and J. Ziugszda, *Heat Transfer of Cylinder in Cross Flow of Fluid.* Academy of Sciences of the Lithuanian SSR, Inst. Phys. and Tech. Problems of Energetics, Vilnius (1979).
8. V. Gnielinski, Berechnung mittlerer Wärme- und Stoffübergangskoeffizienten an laminar und turbulent überströmten Einzelkörpern mit Hilfe einer einheitlichen Gleichung, *Forsch. Ing. Wesen* **41,** 145–153 (1975).
9. W. Kast, O. Krischer, H. Reinicke and K. Wintermantel, *Konvektive Wärme- und Stoffübertragung.* Springer-Verlag, Berlin (1974).
10. *VDI-Wärmeatlas*, Chaps. Ge 1–Gf 3; C. Ld 1–Ld 7. Verein Deutscher Ingenieure, VDI-Verlag (1984).

TRANSFERT THERMIQUE ET PERTE DE CHARGE, COTE CALANDRE, DE TUBES AYANT UNE FORME OVALE

Résumé—On étudie expérimentalement le transfert thermique et la perte de charge d'un écoulement croisé autour d'un arrangement de tubes ayant différents pass transversaux et longitudinaux respectivement dans le domaine $1{,}97 \leqq t_q \leqq 3{,}16$ et $0{,}67 \leqq t_l \leqq 1{,}0$. Le transfert thermique est déterminé à l'aide de l'analogie entre transferts de masse et de chaleur, à partir de mesures sur la diffusion du naphtalène. Les résultats montrent que les échangeurs avec une section ovale ont des sections frontales considérablement plus petites, côté calandre, que ceux avec des tubes circulaires.

WÄRMEÜBERGANG UND DRUCKVERLUST AUF DER AUßENSEITE QUER AUGESTRÖMTER ROHRBÜNDEL MIT OVALEN ROHREN

Zusammenfassung—Wärmeübergang und Druckverlust der Strömung auf der Außenseite in versetzt angeordneten Rohrbündeln mit unterschiedlichen Quer- und Längsteilungen im Bereich $1{,}97 \leqslant t_q \leqslant 3{,}16$ und $0{,}67 \leqslant t_l \leqslant 1{,}0$ wurden experimentell bestimmt. Der Wärmeübergang wurde dabei mit Hilfe der Analogie zwischen Wärme- und Stoffübergang aus dem Stoffübergang von Naphthalin in Luft an Testrohren aus Naphthalin bestimmt. Die Ergebnisse zeigen, daß Wärmeübertrager mit Ovalrohren wesentlich kleinere Frontflächen auf der Seite der Außenströmung haben als solche mit Kreisrohren.

ТЕПЛОПЕРЕНОС И ПАДЕНИЕ ДАВЛЕНИЯ В ТЕПЛООБМЕННИКЕ ИЗ ПУЧКОВ ТРУБ, ИМЕЮЩИХ ОВАЛЬНУЮ ФОРМУ

Аннотация—Экспериментально изучается теплоперенос и падение давления при поперечном обтекании пучка труб в кожухе теплообменника, расположенных в шахматном порядке, имеющих различные поперечные и продольные шаги в диапазонах $1{,}97 \leqslant t_q \leqslant 3{,}16$ и $0{,}67 \leqslant t_l \leqslant 0{,}1$, соответственно. Теплообмен определялся с использованием аналогии между тепло-и массопереносом путем измерения массовой диффузии нафталина. Результаты показывают, что теплообменники с овальными трубами имеют значительно меньшие фронтальные поверхности по сравнению с теплообменниками из круглых труб.